symmetry

MDPI

Article

A Novel Centrosymmetric Fe(III) Complex with Anionic *Bis*-pyrazolyl-*s*-triazine Ligand; Synthesis, Structural Investigations and Antimicrobial Evaluations

Saied M. Soliman [1,*], Hessa H. Al-Rasheed [2,*], Sobhy E. Elsilk [3] and Ayman El-Faham [1,2]

[1] Department of Chemistry, Faculty of Science, Alexandria University, Ibrahimia, P.O. Box 426, Alexandria 21321, Egypt; aelfaham@ksu.edu.sa
[2] Department of Chemistry, College of Science, King Saud University, P.O. Box 2455, Riyadh 11451, Saudi Arabia
[3] Bacteriology Unit, Botany Department, Faculty of Science, Tanta University, Tanta 31527, Egypt; sobhy.elsilk@science.tanta.edu.eg
* Correspondence: saeed.soliman@alexu.edu.eg or saied1soliman@yahoo.com (S.M.S.); halbahli@ksu.edu.sa (H.H.A.-R.); Tel.: +20-111-136-1059 (S.M.S.); +966-114-673-195 (H.H.A.-R.)

Abstract: Reaction of 2,4-bis(3,5-dimethyl-1*H*-pyrazol-1-yl)-6-methoxy-1,3,5-triazine (**MBPT**) pincer ligand with $FeCl_3$ in acidic medium (1:1 *v*/*v*) afforded the [Fe(BPT)Cl_2(CH_3OH)] complex of the hydrolyzed monobasic ligand: 4,6-bis(3,5-dimethyl-1*H*-pyrazol-1-yl)-1,3,5-triazin-2(1*H*)-one (**HBPT**). In this complex, the Fe(III) ion is hexacoordinated with one anionic pincer ligand unit (**BPT^{-1}**), two chloride ions, and one coordinated methanol molecule. It crystallized in the monoclinic crystal system and centrosymmetric $P2_1/c$ space group with Z = 2 and unit cell parameters of a = 7.309(2) Å, b = 25.461(8) Å, c = 9.918(3) Å and β = 102.646(7)°. The structure of this complex is stabilized by C–H … Cl intramolecular hydrogen bonding interactions with donor acceptor distances ranging from 3.577(3)–3.609(3) Å while its supramolecular structure is controlled by intermolecular O–H … O, O–H … N, and C–H … Cl hydrogen bonding interactions. Hirshfeld analysis of molecular packing indicates that the percentages of the Cl … H, C … O, O … H, C … C, H … C, and N … H contacts are 21.1, 1.7, 10.2, 2.1, 8.6, and 10.4%, respectively. The nature and relative strength of the different coordination interactions in the [Fe(BPT)Cl_2(CH_3OH)] complex are discussed based on atoms in molecules theory. Antimicrobial evaluations indicated that the [Fe(BPT)Cl_2(CH_3OH)] complex showed moderate antibacterial and antifungal activities compared to amoxicillin and ampicillin antibiotics as standard drugs.

Keywords: pincer; Fe(III); hydrolysis; Hirshfeld; antimicrobial activity; anionic bis-pyrazolyl-*s*-triazine

Citation: Soliman, S.M.; Al-Rasheed, H.H.; Elsilk, S.E.; El-Faham, A. A Novel Centrosymmetric Fe(III) Complex with Anionic *Bis*-pyrazolyl-*s*-triazine Ligand; Synthesis, Structural Investigations and Antimicrobial Evaluations. *Symmetry* **2021**, *13*, 1247. https://doi.org/10.3390/sym13071247

Academic Editor: György Keglevich

Received: 29 June 2021
Accepted: 10 July 2021
Published: 12 July 2021

1. Introduction

Iron is considered as a readily available and cheap element with little hazardous effects on the environment. Iron-containing compounds play a crucial role in ammonia production by the Haber–Bosch process and in homogenous molecular catalysis [1–4]. Iron has a great importance in a variety of biological systems of mammals and other simple microorganisms. Generally, it is considered to have low toxicity, but high iron concentrations in living cells can cause some harmful effects, as can iron deficiency [5–7]. High iron levels in the body can catalyze the generation of harmful free radicals [8,9]. In this regard, powerful chelators can be used to control this risk by controlling iron reactivity. Also, iron (III) complexes with N-donor ligands have been reported to have promising anticancer activity [10–13].

2,4-bis(3,5-dimethyl-1*H*-pyrazol-1-yl)-6-methoxy-1,3,5-triazine (**MBPT**, Figure 1) pincer ligand is a powerful nitrogen tridentate chelator that can form metal complexes by the reaction with a diversity of metal salts [14–16]. The self-assembly of this functional ligand with metal salts such as Ni(II), Mn(II), Co(II), Zn(II) and Cd(II) comprising different anions (Cl^-, NO_3^-, ClO_4^-) has afforded a variety of mononuclear homo and heteroleptic metal

(II) complexes with coordination numbers varying from five to eight [14–16]. Using the same technique, the same ligand underwent metal ion-mediated hydrolysis in the presence of $CuCl_2$ or $Cu(ClO_4)_2$, leading to the formation of one-dimensional Cu(II) coordination polymers [17]. Similar hydrolytic reactions were detected in the presence of other metal (II) salts such as $ZnCl_2$, $PdCl_2$, and $PtCl_2$ [15,16,18]. It was confirmed that the role of the metal ion is to increase the acidity of the water molecule, which eases the hydrolytic reaction, as was confirmed by the acid-mediated hydrolysis of **MBPT** in the presence of aqueous hydrochloric acid solution to afford **HBPT** (Figure 1) [17]. In continuation of this work, we tested the reaction of this pincer ligand with $FeCl_3$ in acidic medium. The structure of the new $[Fe(BPT)Cl_2(CH_3OH)]$ complex was confirmed using elemental analysis, FTIR spectra, and single crystal X-ray diffraction. Evaluation of the antimicrobial activity of the studied complex was also presented.

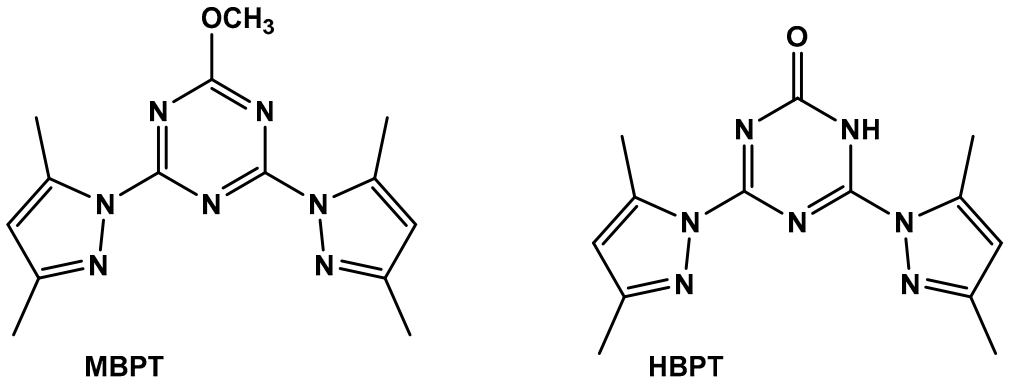

Figure 1. Structure of the **MBPT** ligand and its hydrolyzed product (**HBPT**).

2. Materials and Methods

2.1. Materials and Physical Measurements

Chemicals were purchased from the Sigma-Aldrich Company (Chemie GmbH, 82024 Taufkirchen, Germany). CHN analyses were performed using a Perkin Elmer 2400 Elemental Analyzer (PerkinElmer, Inc., 940 Winter Street, Waltham, MA, USA). Iron content was determined using the Shimadzu atomic absorption spectrophotometer (AA-7000 series, Shimadzu, Ltd., Tokyo, Japan). An Alpha Bruker spectrophotometer (Billerica, MA, USA) was used to measure the FTIR spectra in KBr pellets (Figure S1, Supplementary Data).

2.2. Synthesis

2.2.1. Synthesis of S-Triazine-Based Ligand

The ligand **MBPT** was prepared as previously reported [14] (Supplementary Data, Method S1, Figures S2 and S3).

2.2.2. Synthesis of $[Fe(BPT)(CH_3OH)Cl_2]$ Complex

The studied complex was synthesized using a self-assembly technique by mixing the acidified aqueous (2 drops of 1:1 v/v HCl) solution of $FeCl_3$ (1 mmol, 162 mg) with an equimolar amount of **MBPT** ligand in ethanol. The mixture was left for slow evaporation and the resulting brown crystals were collected by filtration.

Yield; $C_{18}H_{24}N_8Fe_2Cl_6$, 69%. Anal. Calc. C, 37.95%; H, 4.09%; N, 22.13%; Cl, 16.00%; Fe, 12.60%. Found: C, 37.80%; H, 4.01%; N, 21.98%; Cl, 15.88%; Fe, 12.49%; IR (KBr, cm^{-1}): 3454, 1630, 1606, 1586(Sh), 1475 (Figure S1, Supplementary Data).

2.3. Crystal Structure Determination

The crystal structure of the $[Fe(BPT)(CH_3OH)Cl_2]$ complex was determined by using a Bruker D8 Quest diffractometer employing SHELXTL and SADABS programs [19–21]. Hirshfeld calculations were performed using the Crystal Explorer 17.5 program [22–26].

2.4. Antimicrobial Studies

The antimicrobial activities of the [Fe(BPT)(CH_3OH)Cl_2] complex against different microbes were determined following the reported method [27]. More details regarding the antimicrobial assay are found in Supplementary Data (Method S2).

2.5. Atoms in Molecules (AIM) and Natural Charge Calculations

Gaussian 09 [28] software was used for all single point calculations using the MPW1PW91/TZVP [29] method. Charge population and atoms in molecules (AIM) analyses were performed using NBO 3.1 [30] and Multiwfn [31] programs, respectively. Based on literature, *s*-triazine pincer ligands are well known to have a weak ligand field and form only high spin complexes due to the electron-deficient characters of the *s*-triazine moiety. Hence, the calculations were performed based on the fact that the presented complex was a high spin iron (III) complex with a total spin of 5/2 and sextet multiplicity [14].

3. Results

Reaction of the bis-pyrazolyl-*s*-triazine (MBPT) ligand with ferric chloride in acidic medium afforded a novel Fe(III) pincer complex. It was observed that the reaction proceeded with O-demethylation of the methoxy group [32,33] and furnished the hydroxy-*s*-triazine derivative 4,6-bis(3,5-dimethyl-1*H*-pyrazol-1-yl)-1,3,5-triazin-2(1*H*)-one (HBPT), which underwent in situ reaction with $FeCl_3$ and afforded the [Fe(BPT)(CH_3OH)Cl_2] complex in moderate yield. In this complex, the hydrolyzed ligand (HBPT) acted as a mononegative tridentate *NNN*-pincer chelate (Scheme 1). The structure of the [Fe(BPT)(CH_3OH)Cl_2] was confirmed with the aid of elemental analysis, FTIR spectra, and single crystal X-ray diffraction.

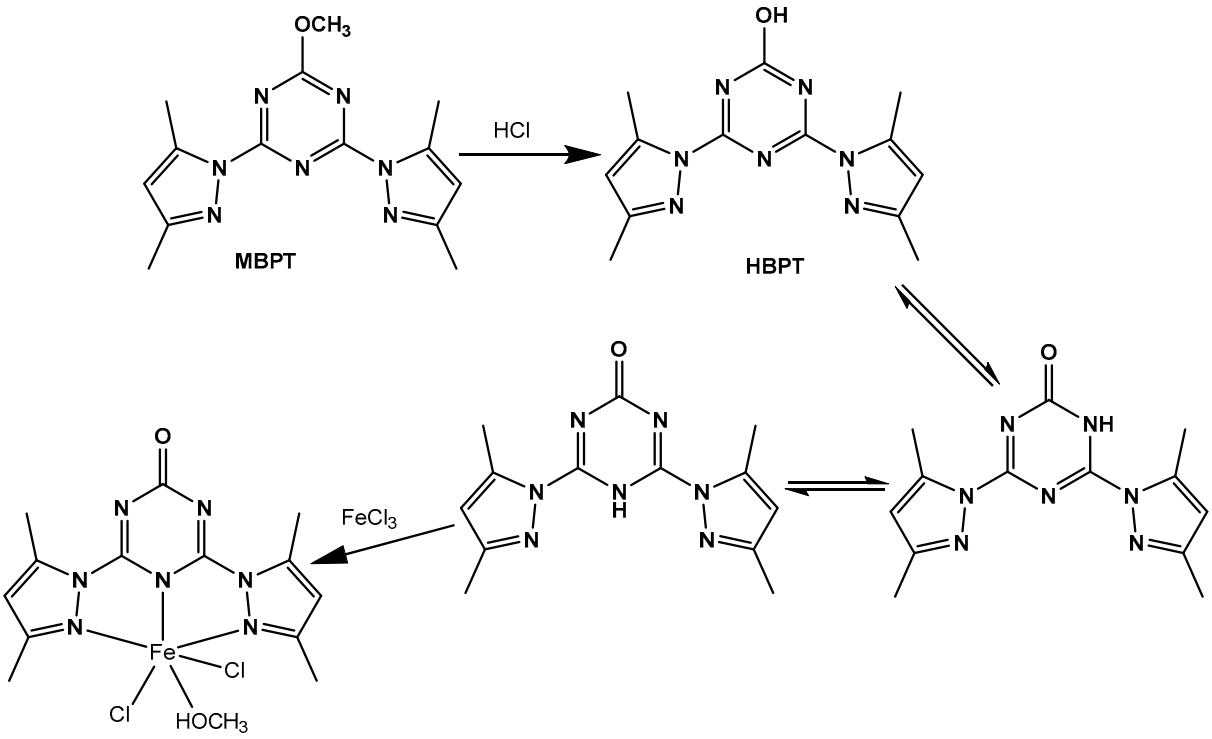

Scheme 1. Reaction of MBPT with $FeCl_3$ in acidic medium.

4. Discussion

4.1. Structure Description

The molecular structure of the heteroleptic [Fe(BPT)(CH_3OH)Cl_2] complex is shown in Figure 2. This Fe(III) complex crystallized in the monoclinic crystal system and $P2_1/c$ space

group with Z = 2 and unit cell parameters of a = 7.309(2) Å, b = 25.461(8) Å, c = 9.918(3) Å, and β = 102.646(7)°, where the asymmetric unit contained one molecular formula. The most relevant geometric parameters are listed in Table 1.

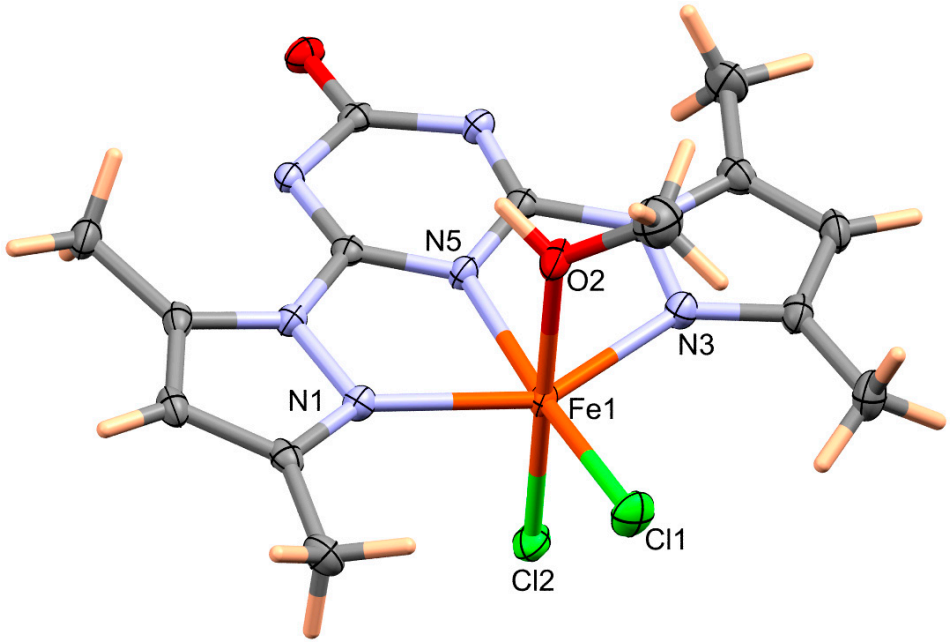

Figure 2. Structure and atom numbering of the [Fe(BPT)(CH_3OH)Cl_2] complex.

Table 1. Crystal data and structure refinement for the [Fe(BPT)(CH_3OH)Cl_2] complex.

Empirical formula	$C_{14}H_{18}Cl_2FeN_7O_2$	
Formula weight	443.10 g/mol	
Temperature	115(2) K	
Wavelength	0.71073 Å	
Crystal system	monoclinic	
Space group	$P2_1/c$	
Unit cell dimensions	a = 7.309(2) Å	α = 90°
	b = 25.461(8) Å	β = 102.646(7)°
	c = 9.918(3) Å	γ = 90°
Volume	1800.9(9) $Å^3$	
Z	4	
Density (calculated)	1.634 g/cm^3	
Absorption coefficient	1.160 mm^{-1}	
F(000)	908	
Crystal size, mm^3	0.18 × 0.19 × 0.22	
Theta range for data collection	2.25 to 25.30°	
Index ranges	$-8 \leq h \leq 8$, $-30 \leq k \leq 30$, $-11 \leq l \leq 11$	
Reflections collected	20,165	

Table 1. *Cont.*

Independent reflections	3277 [R(int) = 0.0346]
Completeness to theta	99.90%
Refinement method	Full-matrix least-squares on F^2
Data/restraints/parameters	3277/0/244
Goodness-of-fit on F^2	1.083
Final R indices [I > 2sigma(I)]	R1 = 0.0339, wR2 = 0.0860
R indices (all data)	R1 = 0.0381, wR2 = 0.0881
Largest diff. peak and hole	1.630 and −0.563
CCDC no.	2090699

In this neutral complex, the Fe(III) was hexacoordinated with a distorted octahedral coordination environment. The Fe(III) was coordinated with one mononegative tridentate $\mathbf{BPT}^{-1}$ and one coordinated chloride ion in the basal plane of the distorted octahedron, while the axial positions were occupied by one chloride anion and a coordinated methanol molecule. Similar to other M(II)–**MBPT** pincer complexes [14–16], there were three Fe–N interactions with the organic pincer ligand where the $Fe–N_{(s\text{-triazine})}$ was generally shorter (Fe1–N5: 2.079(2) Å) than any of the $Fe–N_{(pyrazole)}$ bonds (Fe1–N1: 2.154(2) Å and Fe1–N3: 2.156(2) Å). The equatorial Fe1–Cl1 (2.255(8) Å) was slightly shorter than the axial Fe1–Cl2 (2.302(9) Å), while the Fe1–O2 bond with the coordinated methanol was 2.112(2) Å. As calculated by the continuous shape measure (CShM) tool, the values of the CShM were 2.45 and 13.72 against the perfect octahedron and trigonal prism, respectively indicating a slightly distorted octahedral rather than a trigonal prism [34–37]. The triazine ring itself was not perfectly planar as indicated from the torsion angles where the maximum deviation from planarity was 7.4(3)° for C11–N6–C13–N7 atoms. The mean plane passing through the triazine ring created angles of 2.96 and 7.24° with the pyrazolyl moieties N4C8C7C6N3 and C3C2C1N1N2, respectively. The reason for these twists could be attributed to the small size of Fe(III) and its high charge density, along with the steric hinder between the coordinated pyrazolyl moieties [15].

The structure of this complex was stabilized by C4–H4C ... Cl1 and C9–H9B ... Cl1 intramolecular hydrogen bonds with donor acceptor distances of 3.609(3) and 3.577(3) Å, respectively. On the other hand, its supramolecular structure was controlled by intermolecular O2–H2A ... O1, O2–H2A ... N6, C2–H2 ... Cl2, and C14–H14C ... Cl2 hydrogen bonding interactions with donor acceptor distances of 2.694(3), 3.181(3), 3.605(3), and 3.735(4) Å, respectively. A list of hydrogen bond details is given in Table 2. In addition, presentation of the packed molecular units via these noncovalent interactions is shown in Figure 3.

4.2. Quantitative Analysis of Molecular Packing

Hirshfeld analysis is a simple tool to investigate the molecular packing in the crystal structure at both the qualitative and quantitative levels. In d_{norm} surfaces shown in Figure 4, there were many red regions representing contacts with shorter distances than the van der Waals radii (vdWs) sum of the interacting atoms. On the other hand, the blue and white regions were related to intermolecular contacts having longer and equal interaction distances than the vdWs radii sum of the interacting atoms, respectively. For simplicity, the most significant contacts are labeled A to F, which correspond to Cl ... H, C ... O, O ... H, C ... C, H ... C, and N ... H interactions, respectively.

The hydrogenic H . . . H intermolecular interactions were the most abundant among the other contacts. They contributed 40.9% to the whole fingerprint area (Figure S4; Supplementary Data). There were no red regions related to the H . . . H interactions, indicating longer or equal distances compared to twice the vdW radii of hydrogen atoms. On the other hand, the percentage contributions of the Cl . . . H, C . . . O, O . . . H, C . . . C, H . . . C, and N . . . H contacts were quite less. Their percentages were 21.1, 1.7, 10.2, 2.1, 8.6, and 10.4%, respectively. All these contacts appeared as red regions in the d_{norm} map (Figure 4).

Table 2. Bond lengths (Å) and angles (°) for the [Fe(BPT)(CH_3OH)Cl_2] complex.

Bond	**Distance**	**Bond**	**Distance**
Fe1–N5	2.079(2)	Fe1–N3	2.156(2)
Fe1–O2	2.112(2)	Fe1–Cl1	2.2550(8)
Fe1–N1	2.154(2)	Fe1–Cl2	2.3020(9)
Bond	**Angle**	**Bond**	**Angle**
N5–Fe1–O2	83.02(8)	N1–Fe1–Cl1	106.04(6)
N5–Fe1–N1	73.31(8)	N3–Fe1–Cl1	106.46(6)
O2–Fe1–N1	86.24(8)	N5–Fe1–Cl2	93.35(6)
N5–Fe1–N3	73.02(8)	O2–Fe1–Cl2	175.69(6)
O2–Fe1–N3	85.46(8)	N1–Fe1–Cl2	94.96(6)
N1–Fe1–N3	146.04(8)	N3–Fe1–Cl2	91.28(7)
N5–Fe1–Cl1	170.77(6)	Cl1–Fe1–Cl2	95.87(3)
O2–Fe1–Cl1	87.76(6)		
Fe1–N5	2.079(2)	Fe1–N3	2.156(2)
Fe1–O2	2.112(2)	Fe1–Cl1	2.2550(8)
Fe1–N1	2.154(2)	Fe1–Cl2	2.3020(9)

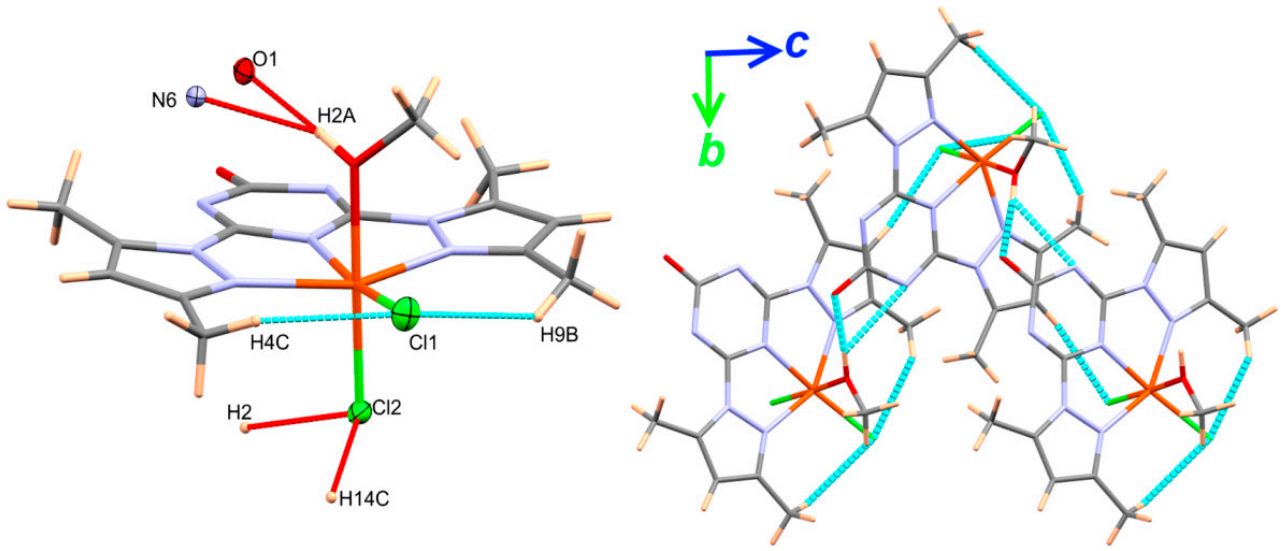

Figure 3. Most important intra- and intermolecular contacts (**left**) and packing scheme (**right**) of the [Fe(BPT)(CH_3OH)Cl_2] complex.

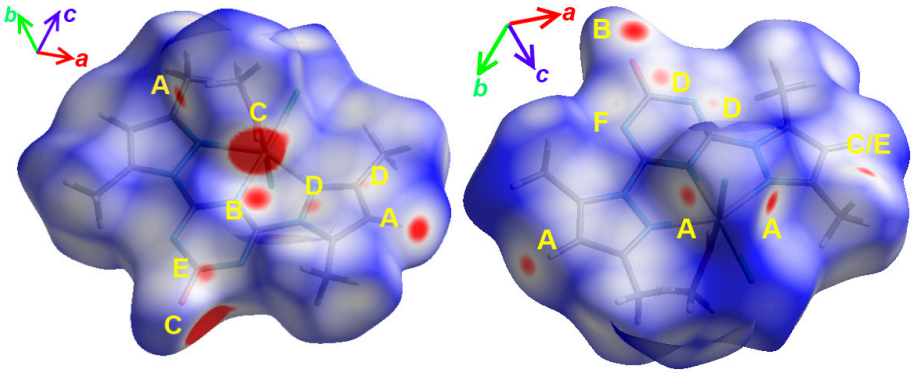

Figure 4. Hirshfeld d_{norm} surfaces showing the different intermolecular interactions; A: Cl . . . H, B: C . . . O; C: O . . . H; D: C . . . C; E: H . . . C, and F: N . . . H contacts.

The shortest contact distances were 2.656Å (Cl2 . . . H2), 3.056 Å (C11 . . . O1), 1.714 Å (O1 . . . H2A), 2.685 Å (H4A . . . C13), 3.331 Å (C13 . . . C3), and 2.615 Å (N7 . . . H5A). A summary of these short contacts and their interaction distances is found in Table 3. In the fingerprint plots shown in Figure 5, the d_e and d_i are distances from a point on the surface to the nearest nucleus *outside* and *inside* the surface, respectively. Hence, the pattern of the fingerprint plot gives strong indication of the strength of interaction. The majority of these interactions appeared as sharp spikes in their fingerprint plots, indicating that these contacts were the most important and had short interaction distances (Figure 5). Also, the total area of the fingerprint plot represents the percentage of the intermolecular interactions that occurred in the crystal. As a result, the decomposition of the fingerprint plot shown in Figure 5 gives the percentages of each intermolecular interaction (Figure S4; Supplementary Data).

Table 3. Summary of the intermolecular interactions and the corresponding shortest interaction distances.

Contact	Distance	Contact	Distance
O1 . . . H2A	1.714	C11 . . . O1	3.056
O1 . . . H4A	2.595	Cl1 . . . H9C	2.814
H4A . . . C13	2.685	Cl2 . . . H2	2.656
C11 . . . C2	3.373	Cl2 . . . H7	2.713
C13 . . . C3	3.331	Cl2 . . . H14C	2.685
N7 . . . H5A	2.615		

4.3. NBO and AIM Studies

The natural charges of the ligand groups and the iron atom were calculated in order to determine the number of charge transferences from the ligand groups as Lewis bases to the Fe(III) as Lewis acid. The charge at the Fe atom decreased to 0.9509 e instead of +3 for the isolated Fe(III) ion. Hence, the amount of negative electron density transferred to Fe(III) from the ligand groups was 2.0492 e. The equatorial chloride (0.5571 e) transferred higher negative electron density to the Fe(III) than the axial one (0.5913 e). The amount of electron density transferred from the mononegative tridentate organic *N*-chelate to the Fe(III) was 0.7424 e, while the corresponding value for the coordinated methanol was 0.1583 e.

On the other hand, the atom–atom interactions could be classified into two main categories, which were the closed shell and sharing interactions [38–41]. Based on the topology analysis of the atoms in molecules (AIM) theory presented in Table 4, the Fe–$N_{(s\text{-triazine})}$ bond (Fe1–N5) had higher electron density (ρ(r)) than any of the Fe–$N_{(pyrazole)}$ bonds (Fe1–N1 and Fe1–N3). Hence, the Fe–$N_{(s\text{-triazine})}$ was stronger and with higher covalent characters than the Fe–$N_{(pyrazole)}$ bonds, which was further confirmed by the negative H(r) values and V(r)/G(r) > 1. In contrast, the Fe–O bond with the coordinated

methanol had low ρ(r), positive H(r) value, and V(r)/G(r) ~ 1, indicating little covalent character of this bond [38–41].

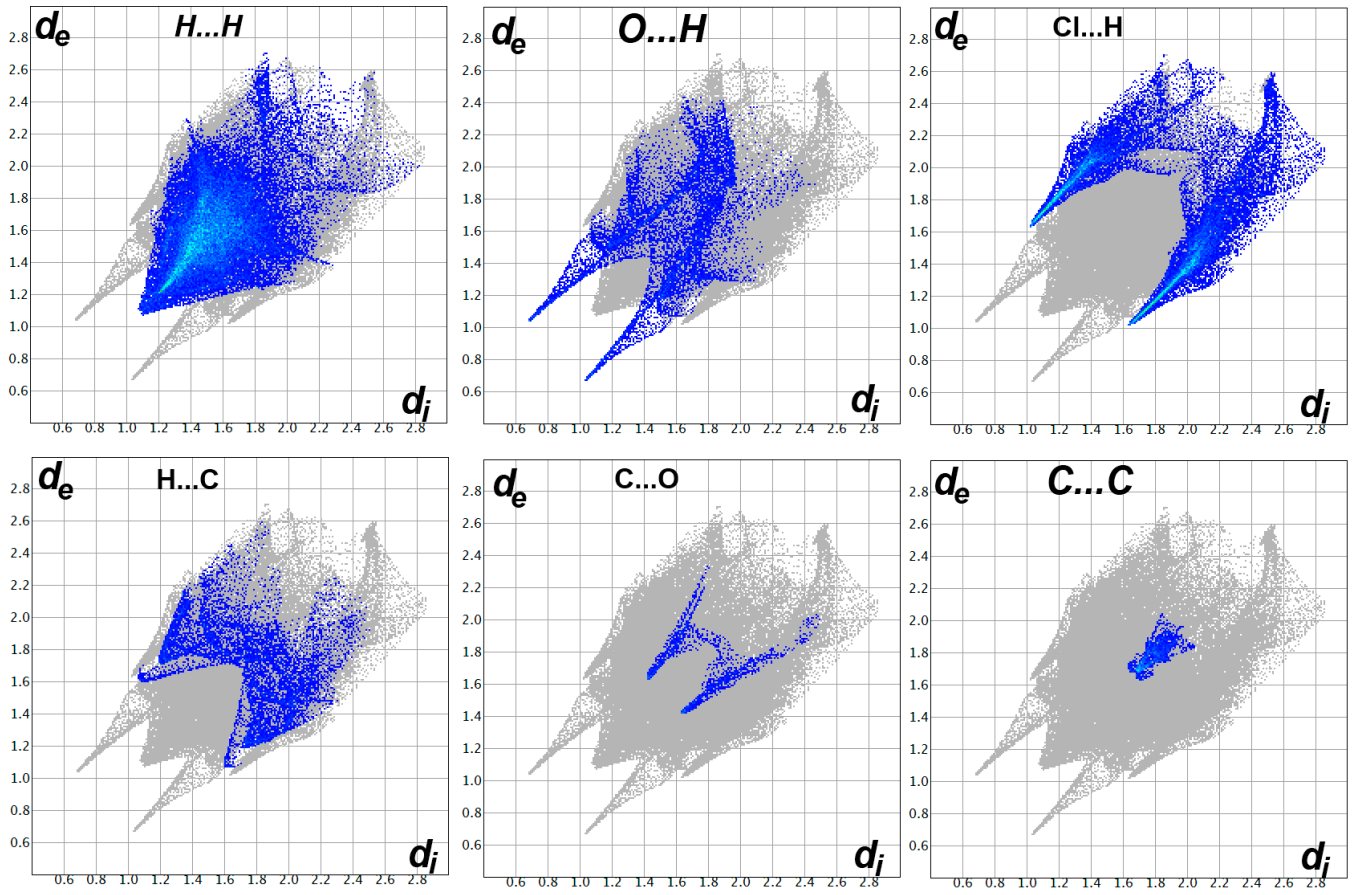

Figure 5. Decomposed fingerprint plots of the most important interactions.

Table 4. Atoms in molecules topology parameters of the [Fe(BPT)(CH_3OH)Cl_2] complex.

Bond	ρ(r)	G(r) [a]	V(r) [b]	E_{int}	H(r) [c]	V(r)/G(r)
Fe1–N5	0.0810	0.1030	−0.1250	39.21	−0.0220	1.21
Fe1–N1	0.0584	0.0728	−0.0803	25.21	−0.0075	1.10
Fe1–N3	0.0580	0.0715	−0.0787	24.70	−0.0072	1.10
Fe1–Cl1	0.0720	0.0730	−0.0898	28.18	−0.0168	1.23
Fe1–Cl2	0.0687	0.0597	−0.0762	23.91	−0.0165	1.28
Fe1–O2	0.0421	0.0795	−0.0791	24.82	0.0004	0.99

[a] Kinetic energy density (a.u.). [b] Potential energy density (a.u.). [c] Total energy density (a.u.).

4.4. Antimicrobial Studies

The biological activity of the [Fe(BPT)(CH_3OH)Cl_2] complex was evaluated against selected Gram-positive (*Staphylococcus aureus*, *Bacillus cereus*, and *Bacillus subtilis*) and Gram-negative (*Escherichia coli* and *Pseudomonas aeruginosa*) bacteria as well as the fungus *Candida albicans*. The inhibition zone diameters were found to be in the range 0.9–1.0 mm at 10 μg/mL of the [Fe(BPT)(CH_3OH)Cl_2] complex. Similar Fe(III) complexes with mono- and bis-pyrazolyl *s*-triazine ligands showed larger inhibition zone diameters (12–25 mm) against the same microbes [42]. It is worth concluding that the antimicrobial activities depend not only on the ligand and nature of the coordination environment around the metal ion but also on the type of substituent attached to the triazine moiety.

In addition, the Minimum Inhibitory Concentrations (MICs) were determined against these microbes (Table 5). The results indicated broad spectrum antimicrobial action against

these microbes with MIC values of 6.8, 9.7, 7.3, 7.9, 7.3, and 6.2 mM/L. The results indicated moderate antibacterial and antifungal actions of the [Fe(BPT)(CH_3OH)Cl_2] complex compared to the standard antibiotics amoxicillin and ampicillin.

Table 5. The MIC values (mM/L) of the [Fe(BPT)(CH_3OH)Cl_2] complex against different microbes compared to some antibiotics.

Microbe	[Fe(BPT)(CH_3OH)Cl_2]	Amoxicillin	Ampicillin
St. aureus	6.8	2.7	2.7
B. cereus	7.9	2.1	2.1
B. subtilis	7.3	2.7	3.6
E. coli	7.9	2.7	3.6
P. aeruginosa	7.3	2.1	2.9
C. albicans	6.2	3.4	4.3

5. Conclusions

A new hexacoordinated [Fe(BPT)Cl_2(CH_3OH)] pincer complex was synthesized by the reaction of 2,4-bis(3,5-dimethyl-1*H*-pyrazol-1-yl)-6-methoxy-1,3,5-triazine (**MBPT**) with $FeCl_3$ in acidic medium. During the complexation process in an acidic medium, the O-demethylation of the methoxy group occurred and furnished the hydroxy-*s*-triazine derivative; 4,6-bis(3,5-dimethyl-1*H*-pyrazol-1-yl)-1,3,5-triazin-2(1*H*)-one (**HBPT**). The latter underwent complexation with $FeCl_3$ as an anionic *NNN*-pincer ligand coordinating the Fe(III) by one short Fe–$N_{(s\text{-triazine})}$ and two equidistant Fe–$N_{(pyrazole)}$ bonds. The hexacoordination environment was completed by two chloride ions and one methanol. The [Fe(BPT)Cl_2(CH_3OH)] complex had moderate antimicrobial activity against some selected microbes. Hirshfeld analysis was used to quantify the different intermolecular contacts while atoms in molecules (AIM) topology parameters were used to describe the nature and strength of coordination interactions in the [Fe(BPT)Cl_2(CH_3OH)] complex.

Supplementary Materials: The following are available online at https://www.mdpi.com/article/10.3390/sym13071247/s1, Method S1: Synthesis of MBPT, Method S2: Antimicrobial Studies, Figure S1: FTIR spectra of the [Fe(BPT)(CH_3OH)Cl_2] complex, Figure S2: FTIR spectra of the ligand (MBPT), Figure S3: ^1H and ^{13}C NMR spectra of the ligand (MBPT). Chemical shifts are reported in parts per million (ppm), Figure S4: Summary of the intermolecular interactions and their percentages.

Author Contributions: The work was designed and supervised by S.M.S. X-ray structure analyses were performed by S.M.S. Computational calculations as well as the synthesis of the complex was carried out by S.M.S. S.E.E. performed the antimicrobial investigations. A.E.-F. and H.H.A.-R. carried out the preparations of the organic ligands and their analyses. All authors contributed to the first draft and the final version. All authors have read and agreed to the published version of the manuscript.

Funding: Deanship of Scientific Research at King Saud University funded this research, grant number RG–1441–365, Saudi Arabia.

Institutional Review Board Statement: Not applicable.

Informed Consent Statement: Not applicable.

Data Availability Statement: The data presented in this study are available on request from the corresponding author.

Acknowledgments: The authors extend their thanks to the Deanship of Scientific Research at King Saud University for funding this work through research group no. (RG–1441–365, Saudi Arabia).

Conflicts of Interest: The authors declare no conflict of interest.

References

1. Bolm, C.; Legros, J.; Le Paih, J.; Zani, L. Iron-Catalyzed Reactions in Organic Synthesis. *Chem. Rev.* **2004**, *104*, 6217–6254. [CrossRef] [PubMed]
2. Bauer, I.; Knölker, H.-J. Iron Catalysis in Organic Synthesis. *Chem. Rev.* **2015**, *115*, 3170–3387. [CrossRef] [PubMed]

3. Wei, D.; Darcel, C. Iron Catalysis in Reduction and Hydrometalation Reactions. *Chem. Rev.* **2019**, *119*, 2550–2610. [CrossRef] [PubMed]
4. Ludwig, J.R.; Schindler, C.S. Catalyst: Sustainable Catalysis. *Chemistry* **2017**, *2*, 313–316. [CrossRef]
5. Egorova, K.S.; Ananikov, V.P. Toxicity of Metal Compounds: Knowledge and Myths. *Organometallics* **2017**, *36*, 4071–4090. [CrossRef]
6. Egorova, K.S.; Ananikov, V.P. Which Metals are Green for Catalysis? Comparison of the Toxicities of Ni, Cu, Fe, Pd, Pt, Rh, and Au Salts. *Angew. Chem. Int. Ed.* **2016**, *55*, 12150–12162. [CrossRef]
7. Bauer, E.B. Iron Catalysis II. *Top. Organomet. Chem.* **2015**, *50*, 1–18.
8. Crisponi, G.; Remelli, M. Iron chelating agents for the treatment of iron overload. *Coord. Chem. Rev.* **2008**, *252*, 1225–1240. [CrossRef]
9. Brittenham, G.M. *Hematology: Basic Principles and Practice*; Hoffman, R., Benz, E., Shattil, S., Furie, B., Cohen, H., Eds.; Churchill Livingstone: New York, NY, USA, 1991; p. 327.
10. Graminha, A.E.; Vilhena, F.S.; Batista, A.A.; Louro, S.R.; Ziolli, R.L.; Teixeira, L.R.; Beraldo, H. 2-Pyridinoformamide-derived thiosemicarbazones and their iron(III) complexes: Potential antineoplastic activity. *Polyhedron* **2008**, *27*, 547–551. [CrossRef]
11. Basha, M.T.; Bordini, J.; Richardson, D.R.; Martinez, M.; Bernhardt, P.V. Kinetico-mechanistic studies on methemoglobin generation by biologically active thiosemicarbazone iron(III) complexes. *J. Inorg. Biochem.* **2016**, *162*, 326–333. [CrossRef]
12. Morcelli, S.R.; Kanashiro, M.M.; Candela, D.R.; Alzamora, M.; Horn, A., Jr.; Fernandes, C. Synthesis, characterization and antitumoral activity of new di-iron(III) complexes containing naphthyl groups: Effect of the isomerism on the biological activity. *Inorg. Chem. Commun.* **2016**, *67*, 22–24. [CrossRef]
13. Chaston, T.B.; Lovejoy, D.B.; Watts, R.N.; Richardson, D.R. Examination of the Antiproliferative Activity of Iron Chelators: Multiple Cellular Targets and the Different Mechanism of Action of Triapine Compared with Desferrioxamine and the Potent Pyridoxal Isonicotinoyl Hydrazone Analogue 311. *Clin. Cancer Res.* **2003**, *9*, 402–414. [PubMed]
14. Soliman, S.M.; El-Faham, A. Synthesis, characterization, and structural studies of two heteroleptic Mn(II) complexes with tridentate N,N,N-pincer type ligand. *J. Coord. Chem.* **2018**, *71*, 2373–2388. [CrossRef]
15. Soliman, S.M.; Almarhoon, Z.; El-Faham, A. Synthesis, Molecular and Supramolecular Structures of New Cd(II) Pincer-Type Complexes with *s*-Triazine Core Ligand. *Crystals* **2019**, *9*, 226. [CrossRef]
16. Soliman, S.M.; Elsilk, S.E.; El-Faham, A. Synthesis, structure and biological activity of zinc (II) pincer complexes with 2,4-*bis*(3,5-dimethyl-1*H*-pyrazol-1-yl)-6-methoxy-1,3,5-triazine. *Inorg. Chim. Acta* **2020**, *508*, 119627. [CrossRef]
17. Soliman, S.M.; Elsilk, S.E.; El-Faham, A. Novel one-dimensional polymeric Cu(II) complexes via Cu(II)-assisted hydrolysis of the 2,4-*bis*(3,5-dimethyl-1*H*-pyrazol-1-yl)-6-methoxy-1,3,5-triazine pincer ligand: Synthesis, structure, and antimicrobial activities. *Appl. Organomet. Chem.* **2020**, *34*, e5941. [CrossRef]
18. Lasri, J.; Haukka, M.; Al-Rasheed, H.H.; Abutaha, N.; El-Faham, A.; Soliman, S.M. Synthesis, Structure and In Vitro Anticancer Activity of Pd(II) Complex of Pyrazolyl-*s*-Triazine Ligand; A New Example of Metal-Mediated Hydrolysis of *s*-Triazine Pincer Ligand. *Crystals* **2021**, *11*, 119. [CrossRef]
19. Sheldrick, G.M. *Program for Empirical Absorption Correction of Area Detector Data*; University of Göttingen: Göttingen, Germany, 1996.
20. Sheldrick, G.M. SHELXT-Integrated space-group and crystal-structure determination. *Acta Cryst. A* **2015**, *71*, 3–8. [CrossRef]
21. Spek, A.L. Structure validation in chemical crystallography. *Acta Cryst. D* **2009**, *65*, 148–155. [CrossRef]
22. Turner, M.J.; McKinnon, J.J.; Wolff, S.K.; Grimwood, D.J.; Spackman, P.R.; Jayatilaka, D.; Spackman, M.A. *Crystal Explorer 17*; University of Western Australia: Perth, Australia, 2017. Available online: http://hirshfeldsurface.net (accessed on 12 June 2017).
23. Spackman, M.A.; Jayatilaka, D. Hirshfeld surface analysis. *CrystEngComm* **2009**, *11*, 19–32. [CrossRef]
24. Spackman, M.A.; McKinnon, J.J. Fingerprinting intermolecular interactions in molecular crystals. *CrystEngComm* **2002**, *4*, 378–392. [CrossRef]
25. Bernstein, J.; Davis, R.E.; Shimoni, L.; Chang, N.-L. Patterns in hydrogen bonding: Functionality and graph set analysis in crystals. *Angew. Chem. Int. Ed. Engl.* **1995**, *34*, 1555–1573. [CrossRef]
26. McKinnon, J.J.; Jayatilaka, D.; Spackman, M.A. Towards quantitative analysis of intermolecular interactions with Hirshfeld surfaces. *Chem. Commun.* **2007**, *37*, 3814–3816. [CrossRef]
27. Sharma, A.; Ghabbour, H.; Khan, S.T.; de la Torre, B.G.; Albericio, F.; El-Faham, A. Novel pyrazolyl-s-triazine derivatives, molecular structure and antimicrobial activity. *J. Mol. Struct.* **2017**, *1145*, 244–253. [CrossRef]
28. Frisch, M.J.; Trucks, G.W.; Schlegel, H.B.; Scuseria, G.E.; Robb, M.A.; Cheeseman, J.R.; Scalmani, G.; Barone, V.; Mennucci, B.; Petersson, G.A.; et al. *GAUSSIAN 09. Revision A02*; Gaussian Inc.: Wallingford, CT, USA, 2009.
29. Adamo, C.; Barone, V. Exchange functionals with improved long-range behavior and adiabatic connection methods without adjustable parameters: The mPWmPW and mPW1PWmPW1PW models. *J. Chem. Phys.* **1998**, *108*, 664–675. [CrossRef]
30. Glendening, E.D.; Reed, A.E.; Carpenter, J.E.; Weinhold, F. *NBO Version 3.1, CI*; University of Wisconsin: Madison, WI, USA, 1998.
31. Lu, T.; Chen, F. Multiwfn: A multifunctional wavefunction analyzer. *J. Comput. Chem.* **2012**, *33*, 580–592. [CrossRef]
32. Lucescu, L.; Ghinet, A.; Belei, D.; Rigo, B.; Dubois, J.; Bîcu, E. Discovery of indolizines containing triazine moiety as new leads for the development of antitumoral agents targeting mitotic events. *Bioorg. Med. Chem. Lett.* **2015**, *25*, 3975–3979. [CrossRef]
33. Woods, K.W.; Lai, C.; Miyashiro, J.M.; Tong, Y.; Florjancic, A.S.; Han, E.K.; Soni, N.; Shi, Y.; Lasko, L.; Leverson, J.D.; et al. Aminopyrimidinone Cdc7 Kinase Inhibitors. *Bioorg. Med. Chem. Lett.* **2012**, *22*, 1940–1943. [CrossRef]

34. Ok, K.M.; Halasyamani, P.S.; Casanova, D.; Llunell, M.; Alvarez, S. Distortions in Octahedrally Coordinated d^0 Transition Metal Oxides: A Continuous Symmetry Measures Approach. *Chem. Mater.* **2006**, *18*, 3176–3183. [CrossRef]
35. Santiaqo, A.; David, A.; Llunell, M.; Pinsky, M. Continuous symmetry maps and shape classification. The case of six-coordinated metal compounds. *New J. Chem.* **2002**, *26*, 996–1009.
36. Hagit, Z.; Shmuel, P.; David, A. Continuous symmetry measures. *J. Am. Chem. Soc.* **1992**, *114*, 7843–7851.
37. Keinan, S.; Avnir, D. Quantitative Symmetry in Structure–Activity Correlations: The Near C_2 Symmetry of Inhibitor/HIV Protease Complexes. *J. Am. Chem. Soc.* **2000**, *122*, 4378–4384. [CrossRef]
38. Bobrov, M.F.; Popova, G.V.; Tsirelson, V.G. topological analysis of electron density and chemical bonding in cyclophosphazenes PnN_nX_{2n} (X = H, F, Cl; n = 2, 3, 4). *Russ. J. Phys. Chem.* **2006**, *80*, 584–590. [CrossRef]
39. Gatti, C. Chemical bonding in crystals: New directions. *Z. Kristallogr.* **2005**, *220*, 399–457. [CrossRef]
40. Gibbs, G.V.; Downs, R.T.; Cox, D.F.; Ross, N.L.; Boisen, M.B.; Rosso, K.M., Jr. Shared and closed-shell O-O interactions in silicates. *J. Phys. Chem. A* **2008**, *112*, 3693–3699. [CrossRef] [PubMed]
41. Cremer, D.; Kraka, E. Chemical Bonds without Bonding Electron Density—Does the Difference Electron Density Analysis Suffice for a Description of the Chemical Bond? *Angew. Chem. Int. Ed. Engl.* **1984**, *23*, 627–628. [CrossRef]
42. Soliman, S.M.; Al-Rasheed, H.H.; Albering, J.H.; El-Faham, A. Fe(III) Complexes Based on Mono- and Bis-pyrazolyl-*s*-triazine Ligands: Synthesis, Molecular Structure, Hirshfeld, and Antimicrobial Evaluations. *Molecules* **2020**, *25*, 5750. [CrossRef]